SEBHA UNIVERSITY JOURNAL OF PURE & APPLIED SCIENCES VOL.21 NO. 1 2022
DOI: 10.51984/JOPAS.V21I1.1671

مجلة جامعة سبها للعلوم البحتة والتطبيقية
Sebha University Journal of Pure & Applied Sciences

Journal homepage: www.sebhau.edu.ly/journal/index.php/jopas

Study The Effect of Extract berry and mango leaves as a corrosion inhibitor of Cu, Carbon steel and Oil Pipelines.

*Hamdy AB. Matter[1,2] & Tariq M. Ayad[1]

[1]Chemistry Department, Benghazi University, El-Wahate, Jalou, Libya
[2]High Institute of Engineering and Technology, El-Arish, Egypt

Keywords:
The corrosion
Carbon Steel
Iron
Copper
Oil Pipelines

ABSTRACT

For the corrosion of iron, copper and carbon steel in 1.0 M HCl and 1.0 M of HNO3 solution. The materials extracted from the berry and mango leaves when added in different concentrations to solutions of 1 molar of hydrochloric acid and nitric acid have shown remarkable and effective resistance to corrosion of iron, copper and carbon steel, as well as to the samples that we brought from the oil companies in Galo to study the extent of resistance of these materials to their corrosion and the use of these natural and extracted products of berry leaves and mango leaves for use as corrosion inhibitors for oil pipelines These natural products, which are available in the environment, have shown a great deal of effective resistance to corrosion of oil pipelines. The effect of both the temperature and the concentration of these substances on the corrosion of these minerals has been studied and the study has shown that they inhibit corrosion even at low concentrations of reach to 50 ppm.

دراسة تأثير مستخلص أوراق التوت والمانجو كمانع للتآكل في أنابيب النحاس والصلب الكربوني و أنابيب النفط

*حمدي عبد الباقي مطر [1,2] و طارق محمد عياد [1]

[1]قسم الكيمياء، جامعة بنغازي، الواحات جالو، ليبيا
[2]المعهد العالي للهندسة والتكنولوجيا بالعريش، مصر

الكلمات المفتاحية:
التآكل
الصلب
الحديد
النحاس
أنابيب النفط

الملخص

لقد أظهرت المواد المستخلصة من أوراق التوت وأوراق المانجو عند اضافتها بتركيزات مختلفة إلى محاليل 1 مولاري من حمض الهيدروكلوريك وحمض النيتريك مقاومة ملحوظة وفعالة في مقاومة تآكل الحديد والنحاس والحديد الصلب وكذلك للعينات التي جلبناها من شركات النفط بجالو لدراسة مدى مقاومة هذه المواد لتآكلها واستخدام هذه المنتجات الطبيعية والمستخلصة من أوراق التوت وأوراق المانجو كمثبطات لتآكل أنابيب النفط وقد أظهرت هذه المنتجات الطبيعة والمتوفرة في البيئة بصورة كبيرة مقاومة فعالة لتآكل مواسير النفط. وقد تم دراسة تأثير كلا من تركيز تلك المواد ودرجة الحرارة (25 -45 م) على تآكل تلك المعادن وأظهرت الدراسة أنها تثبط التآكل حتى عند تركيزات منخفضة تصل إلى 50 جزء من المليون ودراسة تأثير كلا من درجة الحرارة والتركيز على كفاءة التثبيط.

1-Introduction

The active interactions between erosion and corrosion processes were confirmed when the mechanical erosion was concentrated on electrochemical corrosion anodes. [1]. The polyurethane / polysiloxane hybrid coating have a two-hundred-fold greater in corrosion induction time due to incorporation of organic inhibitor as, 2-mercaptobenzothiazole (MBT), in polylactic acid (PLA MBT)-impregnated PLA nanoparticles, utilization (EIS) electrochemical impedance spectroscope, and potential-static polarization technique [2]. The formation of reversed austenite at the Cr-depleted regions losses the number of nucleation sites for intergranular corrosion, and the opposite austenite always distributed along the martensite lath boundaries, inhibition the propagation of intergranular corrosion [3]. The electrochemical properties of 7 active aromatic compounds extracted from natural sources like caffeic acid, gallic acid thymol (2-isopropyl-5-methylphenol, (2-hydroxy-1,4-naphthoquinone), (3 ,4,5-trihydroxybenzoic acid), wedelolactone, tannic, and ellagic acid

Corresponding author:
E-mail addresses: hamdy.matter@uob.edu.ly ,(T. M. Ayad1) tariq.ayad@uob.edu.ly

Article History : Received 29 December 2021 - Received in revised form 29 May 2022 - Accepted 19 June 2022

are investigated using nanotube multiwalled carbon modified by glassy-carbon electrode, and studded to primary strengthening to understanding behaviour of their redox at different environmental pH conditions [4]. Discussed and analysed the corrosion renitent (F/M) ferritic/martensitic steel, (AFA) alumina-forming austenitic, (ASS) austenitic stainless steel, (SS) stainless steel, and, (ODS) oxide dispersion strengthened steel in supercritical water [5]. The decrease of graphene caused the corrosion and the galvanic cell accelerated the corrosion on copper substrate which two results in the exfoliation of graphene from Cu substrate, and the failure protection of graphene coating [6]. The internal nitridation is occur when no protective oxides can form at the coating surface, and AlN, and TiN are formed in the Co, Ni, Cr, Al, and Y coating after bioxidant corrosion. [7]. The oxide scale formation rate calculates the overall mechanism of corrosion and the effect of ash deposits on steel. For low-Cr steels the rate oxidation is big and a scale, it is a protective barrier between the deposit and metal surface a few little further oxidations process. The biggest effect of ash on the corrosion procedure was observed for high-Cr steels [8]. To steady Ti as coatings onto AZ91E Mg alloy, used (WS) warm spraying, and followed by post-treatment with epoxy-based polymer resulted in inhabitation of the corrosion performance of Ti warm sprayed coatings [9]. The corrosion rate of the material coatings was affected to the quantity of (GO) graphene oxide present in coating materials. [10]. Effect of piperazine (PZ) degradation on carbon steel corrosion at considerably decrease stripper conditions [11]. Effect of probiotic supplements, which used in orthodontic patients, on corrosion stability of (SS) and 3 types of Ni-Ti orthodontic wires. [12]. Effect of cation type of chloride salts on corrosion behaviour of steel by potentio-dynamic polarization test in concrete powder electrolyte solution in presence of corrosion inhibitors [13]. Al, Cu and Pb may be get into communicate with the cement materials and may be corrode, by loss of weight check of these materials in parts of their corrosion resistance in luting [14]. Fumaria officinalis was used, as a natural inhibitor [15], Nutmeg oil [16], Tannin used as natural corrosion inhibitor for aluminum alloys [17], green tea extract (GT) was used as inhibitor for the corrosion[18], The pectin from tomato peel waste (TPP) was employed as tin corrosion inhibitor[19], tobacco rob extract (TRE) used for Q235 corrosion inhibitor in artificial seawater[20], olive (Olea europaea L) leaf extract, used as corrosion inhibitors for steel in brine solution [21], *Silybum marianum* leaves extract as a 304 stainless steel corrosion inhibitor[22], purple rice bran, extract, used as corrosion inhibitor [23], natural honey with black radish juice, used as corrosion inhibitor of tin[24], and Lupine seeds extract used for steel corrosion inhibitor [25]. "Methyl Carbazodithoate ", was used as the organic compound inhibitor on the corrosion of low carbon steel,[26] and mild steel corrosion. [27] *Theophylline* expired drug, (TD),[28] and, Carbimazole, expired drug, (CD), [29] were used as corrosion inhibitors for mild steel in 0.5M HCl. 3,3-diethyl(4-Chloro)benzoylthiourea, ClDEBT, was used inhibitor on the corrosion of steel in H_2SO_4.[30]

This study was carried out in the city of Jallo, Al-Wahat region - Libya, which are areas rich in oil and petroleum companies. These companies suffer from the problem of erosion of oil pipelines. This research paper wanted to contribute to finding effective and low-cost solutions to solve the problem of corrosion in oil pipelines, so the Arabian Gulf Company cooperated with us and provided us Support by supplying us with samples of the alloys from which oil pipes are made, as well as samples of iron and copper. It was found that extracts of green mango leaves and, berry leaves have high efficincy as corrosion inhibitors.

2- Experimental

2.1. Materials and Chemicals

The carbon steel sheets (supplied from El-khaleeg El-Araby– El-Wahate Oil Company) with the following chemical composition (wt%): C (0.200g), Si (0.003g), Mn (0.35g), P (0.02g) and Fe (Rest). The piece was of dimension1 cm × 1 cm. The sample was embedded in a glass tube of just larger diameter than the sample. Epoxy resin (supplied from Ciba Co.) was used to stick the sample to the glass tube. Surface of carbon steel electrode was mechanically rub off using sand papers, in different grades, for example 1200 grade, before used. The tests were used 1.0 M HCl and, 1.0 M HNO_3 (supplied from Sigma-Aldrich) with the addition of various concentrations of nature products compounds. All the test solutions were prepared from analytical chemistry grade chemical reagents prepared using distilled water, and used without further pure cation. For each hold, a freshly prepared solution was used. Temperature of solutions was thermostatically controlled at desired value, and all chemical material high purity about 99%.

2.2. Extraction of nature products from green berry leaves and green mango leaves

100 g of green berry leaves cutting it a smallest pieces in 1L (DW) distilled water, boiling for 1h leave it to cool, then, filtered and weighed the filtrate extraction, and prepared (300-50) ppm by analytical method it was equal 1g/L =1000 ppm then put 1 ml of extraction filtrate in 20 ml of 1M acid solution then the concentration was 50 ppm and 2ml in 20 ml is equal 100 ppm and so on and also for mango leaves (100g) cutting it a smallest pieces in 1L (DW) distilled water, boiling for 1h leave it to cool, then filtered and weighed the extraction filtrate and prepared (300-50) ppm by analytical method, it was equal 1g/L =1000 ppm then put 1 ml of filtrate in 20 ml of 1M acid solution is 50 ppm and 2ml in 20 ml is equal 100 ppm and so on[18].

2.3. Preparation of acid solutions

HCl (1M) and, HNO_3 (1M) are prepared by analytical method, the volume of acid is divided into 7 bottles 50 ml for bulk solution and 20 ml of six different concentrations of nature extraction inhibitors which extract from nature plants, mango leaves and berry leaves (50-300) ppm for two acids with Cu and Fe alloy of oil pipeline.

3. Results and discussion

3.1. Chemical Method (Weight-Loss Measurements)

Weight loss calculations are comprehensive corrosion tests for laboratory and field. Also, they help us to make a quantitative estimate of amount of corrosion. The corrosion behaviour of the metal in an aqueous environment is describe by the extent to which it dissolves in the water solution.

Calculated the weight of a specimen before and after precipitate and applying the following equation:

$$\Delta W = w_2 - w_1 - - - - - (1)$$

Where w_1 and w_2 are the weights of sample before and after corrosion reaction, respectively. The method depends on the loss of weight is usually perefect method due to the quantity calculated is directly expressed to the amount of corrosion and does not rely on any other assumptions about reactions happening during corrosion.

The value of corrosion rate (CR) was calculated from the following equation:

$$CR = \frac{(\Delta W)}{At} - - - - - (2)$$

Where ΔW was the differences of masses of the specimens before and after corrosion respectively, A is the total area of the specimen (in cm^2) and t is the corrosion time (in min).

Inhibition efficiency percentage (%IE) and the surface coverage (θ) represents that weight of metal surface covered by corrosion with inhibitor molecules were calculated. from the equation (3):

$$\%IE = \frac{CR_0 - CR_i}{CR_0} \times 100 - - - - - - - (3)$$

Where CR_0, and CR_i are corrosion rates without and with inhibitors respectively.

In Fig. (1) show the weight loss-time curves for copper in 1M HNO_3 in the absence and the presence of different concentrations of the extracts, mango inhibitor, and **In Fig. (2,3)** shows the differences between the absence and the presence, respectively, of the mango extraction inhibitor of copper piece in HNO_3 as a corrosion material.

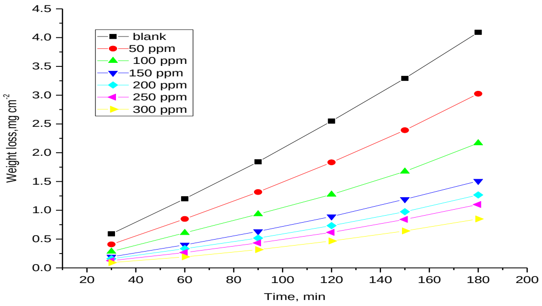

Fig. (1): Show the loss of weight per the time for Cu after corrosion by 1M HNO_3 without and with six different concentrations of mango extract inhibitor.

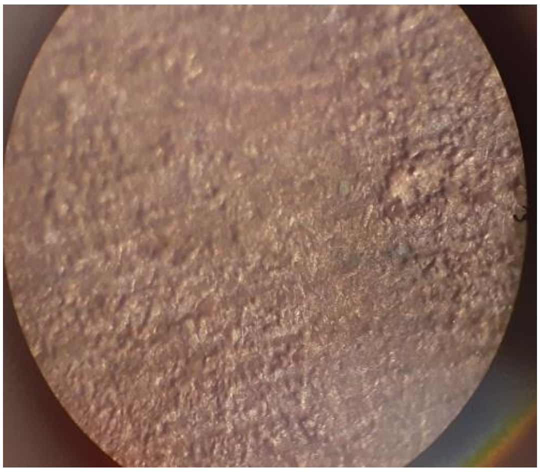

Fig. (2): Show, the corrosion of copper by HNO_3 (1M) without any mango extraction inhibitor.

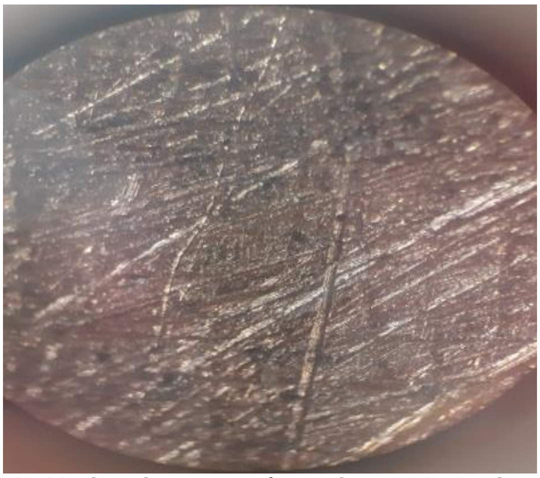

Fig. (3): Show, the corrosion of copper by HNO_3 (1M) with mango extraction inhibitor.

In Fig. (4) show the weight loss-time curves for copper in 1M HNO_3 without and with different concentrations of the extracts, berry inhibitor, and **In Fig. (5,6)** shows the differences between without and with, respectively, of the berry extraction inhibitor of the copper piece in HNO_3 (1M) as a corrosion material.

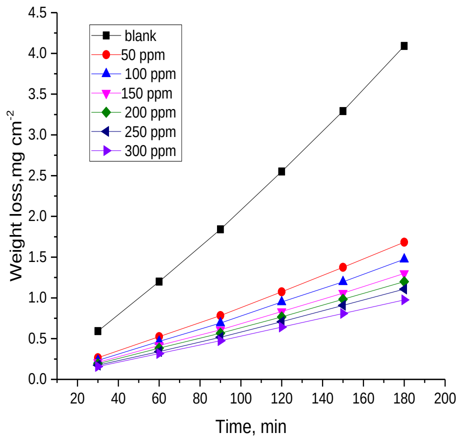

Fig. (4): Show the loss of weight per the time for Cu after corrosion by HNO_3 (1M) without and with six different concentrations of berry extract inhibitor.

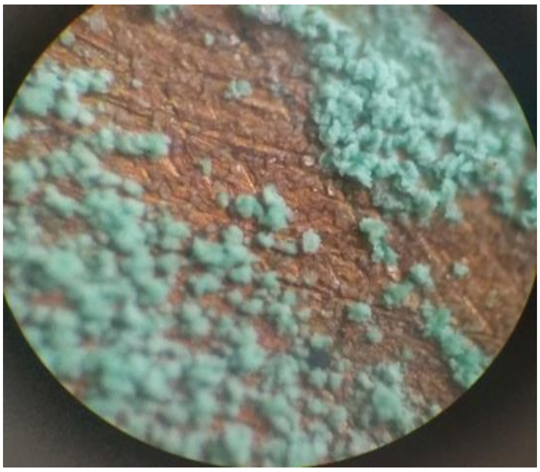

Fig. (5): Show, the corrosion of copper by HNO_3 (1M) without any berry extraction inhibitor.

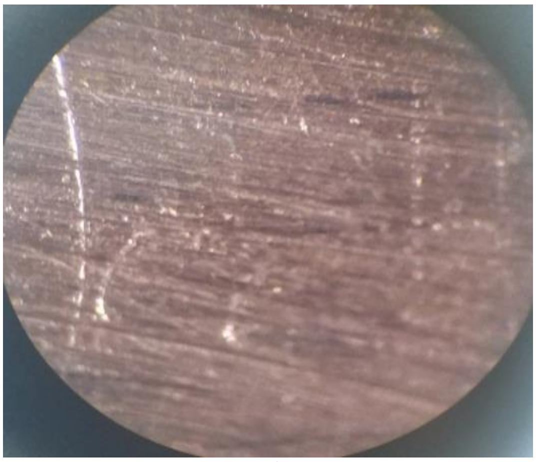

Fig. (6): Show, the corrosion of copper by HNO_3 (1M) with berry extraction inhibitor

It is obvious that loss the weight of copper with berry inhibitor extracts varies linearly with time, and is much lower than that obtained in blank solution. The linearity of curve obtained indicated that an insoluble surface film was absented during corrosion and the extracts were first adsorbed onto the surface of metal and, therefore, hinder the corrosion process. The calculated values of % IE and θ for the investigated inhibitors at 25 °C are listed in **Table (1).** Inspection of the tabulated data showed that, the inhibition efficiency increases by increase the concentration of inhibitor. This behaviour could be attributed to increase the number of adsorbed inhibitors at metal surface.

Table (1): Surface coverage (θ) with inhibition efficiency (%IE) at different concentrations of extracts for the copper corrosion by1M HNO_3. after 90 min.

Concentration, ppm	Mango inhibitor extract		Berry leaves	
	IE%	θ	IE%	θ
50	28.5	0.285	57.5	0.575
100	49.3	0.493	62.4	0.624
150	65.6	0.656	66.9	0.669
200	71.9	0.719	69.2	0.692
250	76.5	0.765	71.9	0.719
300	82.8	0.828	74.2	0.742

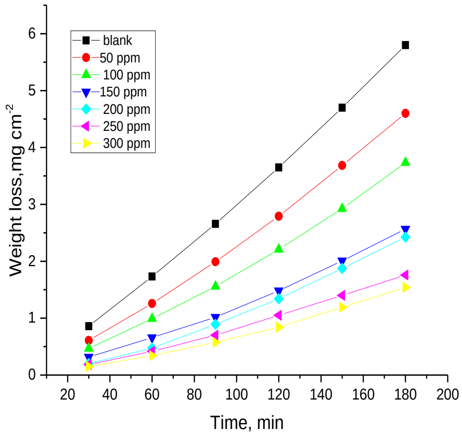

Fig. (7): Show the loss of weight per the time for Cu after corrosion by 1M HCl without and with six different concentrations of mango inhibitor extract.

In Fig. (7) show the weight loss-time curves for Cu in HCl (1M) with and without of different concentrations of the extracts, mango inhibitor, and **In Fig. (8,9)** shows the differences between presence and, absence respectively, of the mango extraction inhibitor of copper piece as a corrosion material by HCl (1M).

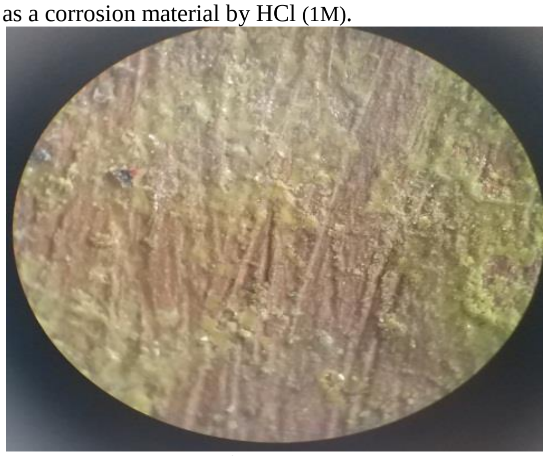

Fig. (8): Show, the corrosion of copper by HCl (1M) without any mango extraction inhibitor.

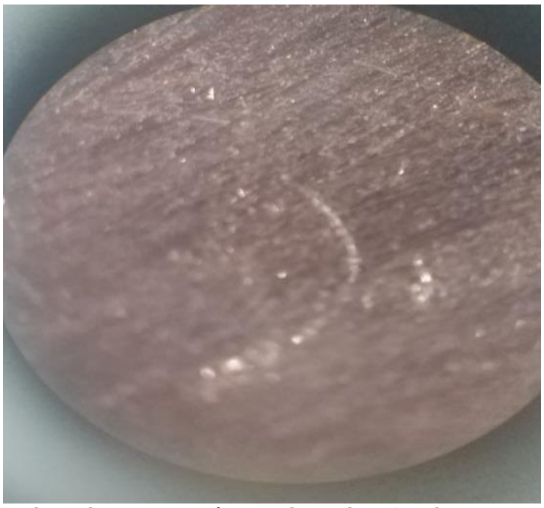

Fig. (9): Show, the corrosion of copper by HCl (1M) with mango extraction inhibitor.

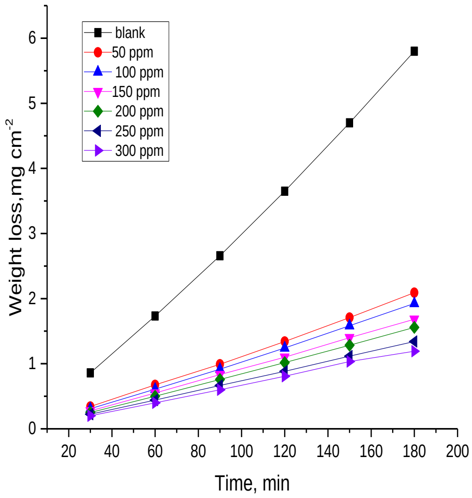

Fig. (10): Show the loss of weight per the time for Cu after corrosion by 1M HCl with and without six different concentrations of berry leaves extract.

In Fig. (10) show the weight loss-time curves for Cu in 1M HCl (1M) without and with different concentrations of the extracts, berry inhibitor, and **In Fig. (11,12)** shows the differences between without and with, respectively of the berry extraction inhibitor of the copper piece in HCl (1M) as a corrosion material.

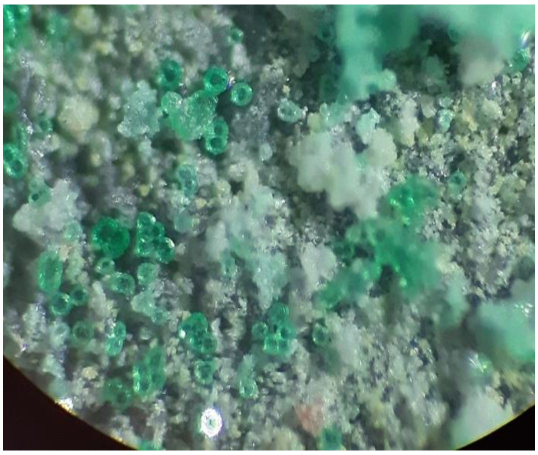

Fig. (11): Show, the corrosion of copper by HCl (1M) without any berry extraction inhibitor.

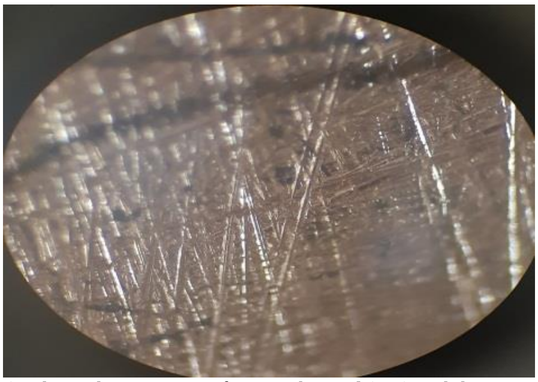

Fig. (12): Show, the corrosion of copper by HCl (1M) with berry extraction inhibitor.

In Fig. (13) show the weight loss-time curves for Fe alloy of oil pipeline in HNO_3 (1M) without and with different concentrations of the extracts, mango inhibitor, and **In Fig. (14,15)** shows the differences between without and with, respectively of the mango extraction inhibitor of the Fe alloy piece in HNO_3 (1M) as a corrosion material.

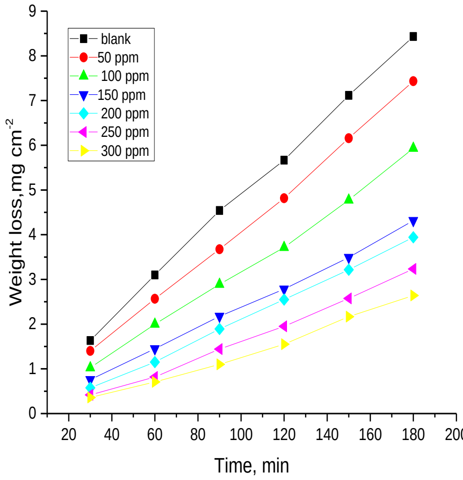

Fig. (13): Show the loss of weight per the time Fe alloy of oil pipeline after corrosion by HNO_3 (1M) without and with six different concentrations of mango inhibitor extract.

Fig. (14): Show, the corrosion Fe alloy of oil pipeline by 1M HNO_3 without mango inhibitor.

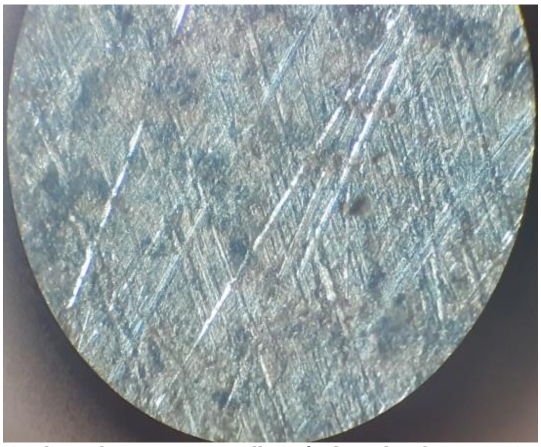

Fig. (15): Show, the corrosion Fe alloy of oil pipeline by HNO_3 (1M) with mango inhibitor.

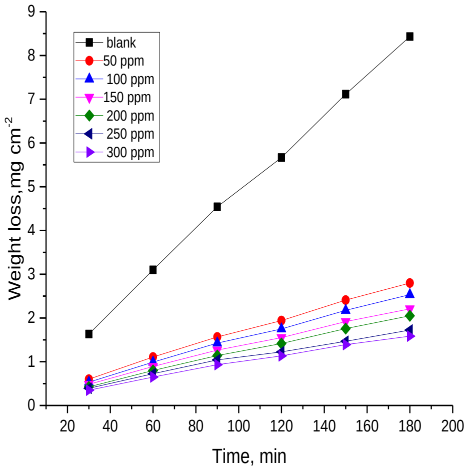

Fig. (16): Show the loss of weight per the time Fe alloy of oil pipeline after corrosion by HNO_3 (1M) without and with six different concentrations berry leaves extract.

In Fig. (16) show the weight loss-time curves for Fe alloy of oil pipeline in HNO_3 (1M) without and with different concentrations of the extracts, berry inhibitor, and **In Fig. (17,18)** shows the differences between without and with, respectively, of the berry extraction inhibitor of the Fe alloy piece in HNO_3 (1M) as a corrosion material.

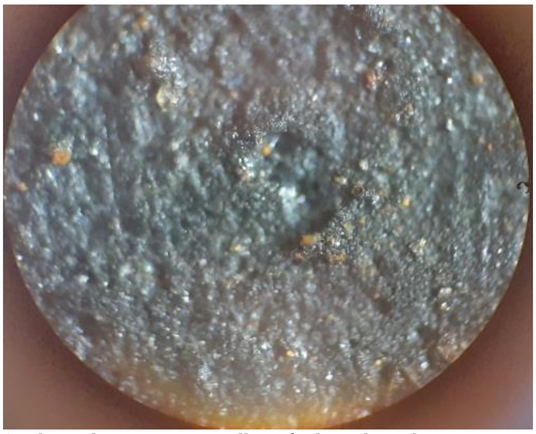

Fig. (17): Show, the corrosion Fe alloy of oil pipeline r by 1M HNO_3 without any berry inhibitor.

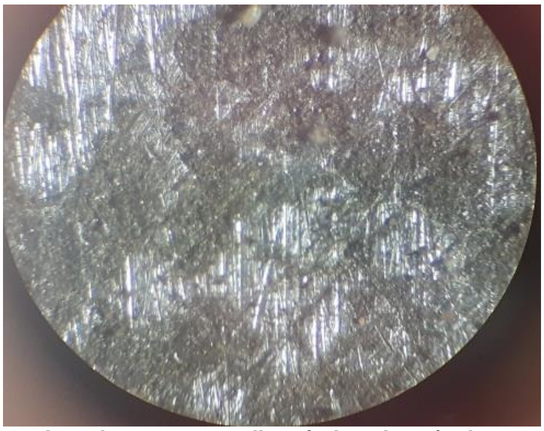

Fig. (18): Show, the corrosion Fe alloy of oil pipeline after by HNO_3 (1M) with berry inhibitor.

In Fig. (19,20) shows the weight loss-time curves for Fe alloy of oil pipeline in HCl (1M) without and with different concentrations of the extracts, mango inhibitor, and berry inhibitor, respectively.

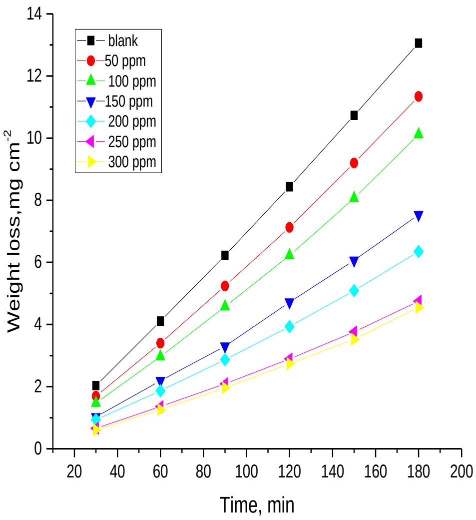

Fig. (19): Show the loss of weight per the time Fe alloy of oil pipeline after corrosion by HCl (1M) without and with six different concentrations of mango inhibitor extract.

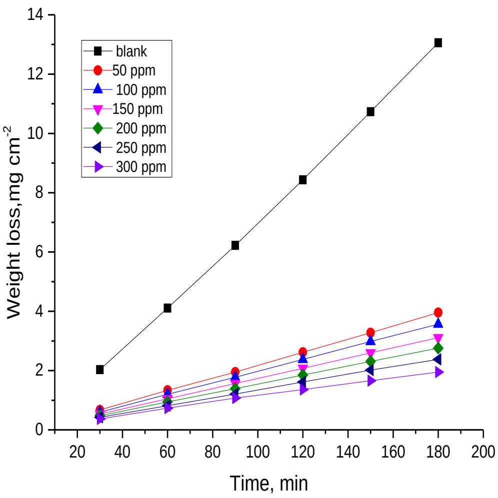

Fig. (20): Show the loss of weight per the time Fe alloy of oil pipeline after corrosion by HCl (1M) without and with six different concentrations of berry leaves extract.

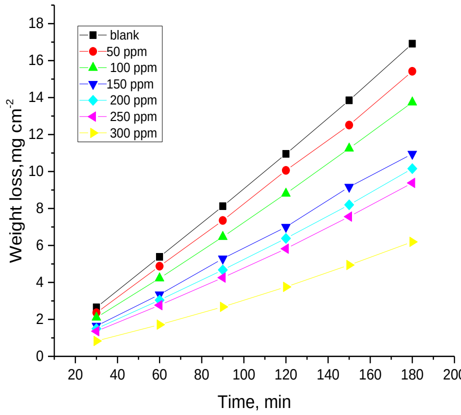

Fig. (21): Show the loss of weight per the time Fe after corrosion by HNO_3 (1M) without and with six different concentrations of mango inhibitor extract.

In Fig. (21) show the weight loss-time curves for Fe in HNO_3 (1M) without and with different concentrations of the extracts, mango inhibitor, and **In Fig. (22,23)** shows the differences between without and with, respectively, of the mango extraction inhibitor of the Fe piece in HNO_3 (1M) as a corrosion material.

Fig. (22): Show, the corrosion of Fe by HNO_3 (1M) without mango inhibitor.

Fig. (23): Show, the corrosion Fe after by HNO_3 (1M) with mango inhibitor.

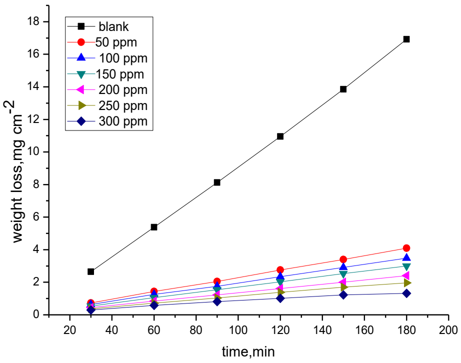

Fig. (24): Show the loss of weight per the time Fe after corrosion by 1M HNO_3 without and with six different concentrations of berry leaves extract.

In Fig. (24) show the weight loss-time curves for Fe in HNO_3 (1M) without and with different concentrations of the extracts, berry inhibitor, and **In Fig. (25,26)** shows the differences between without and with, respectively, of the berry extraction inhibitor of the Fe piece in HNO_3 (1M) as a corrosion material.

Fig. (25): Show Fe after corrosion by HNO_3 (1M) without berry inhibitor.

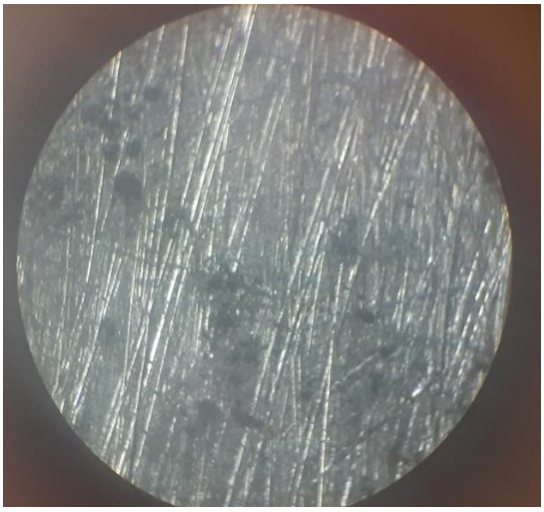

Fig. (26): Show Fe after corrosion by HNO_3 (1M) with berry inhibitor.

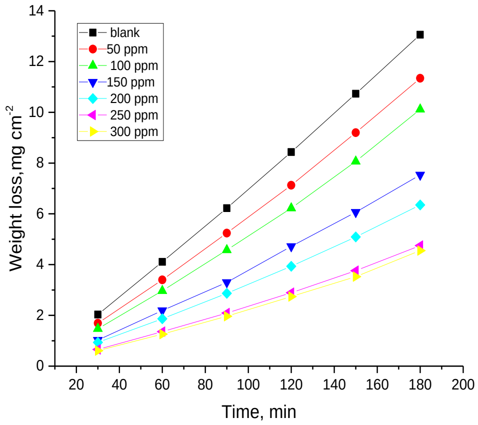

Fig. (27): Show the loss of weight per the time Fe after corrosion by HCl (1M) without and with six different concentrations of mango inhibitor extract.

In Fig. (27) show the weight loss-time curves for Fe in HCl (1M) the absence and presence of different concentrations of the extracts, mango inhibitor, and **In Fig. (28,29)** shows the differences between absence and presence, respectively, of the mango extraction inhibitor of the Fe piece in HCl (1M) as a corrosion material.

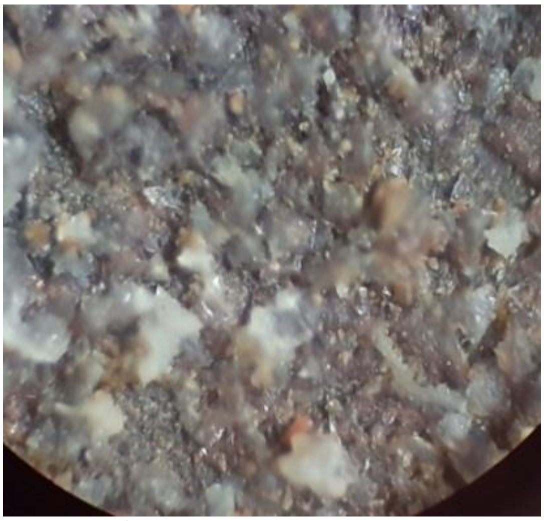

Fig. (28): Show Fe after corrosion by HCl (1M) without mango inhibitor.

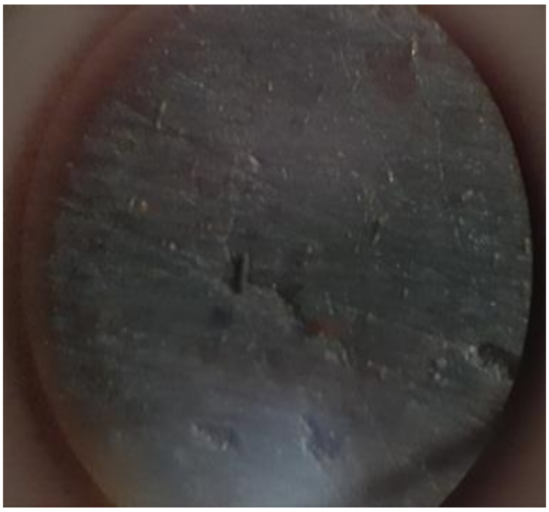

Fig. (29): Show Fe after corrosion by HCl (1M) with mango inhibitor.

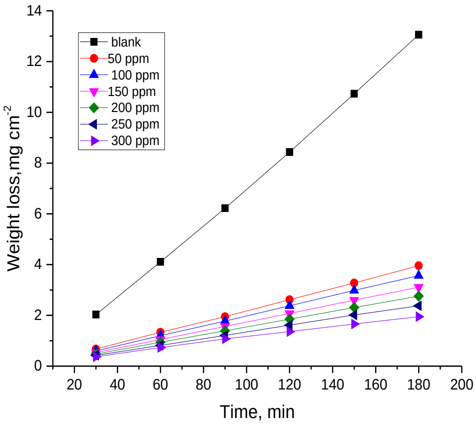

Fig. (30): Show the loss of weight per the time Fe i after corrosion by HCl (1M) without and with six different concentrations of berry leaves extract.

In Fig. (30) show the weight loss-time curves for Fe in HCl (1M) without and with different concentrations of the extracts, berry inhibitor, and **In Fig. (31,32)** shows the differences between without and with, respectively, of the berry extraction inhibitor of the Fe piece in HCl (1M) as a corrosion material.
The more the curves of the inhibitors converge and diverge from the curve of the solution that does not contain the inhibitors, this indicates the efficiency of the inhibitor even at lower concentrations of it, and vice versa.

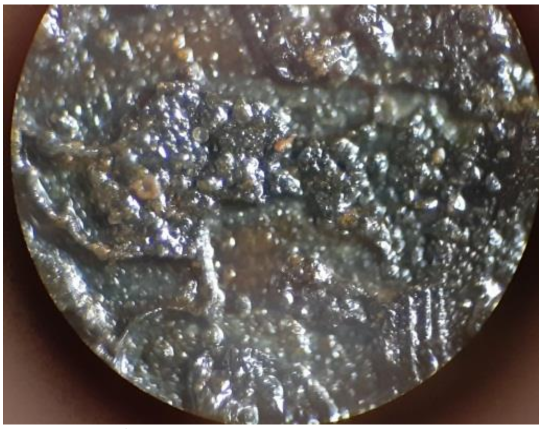

Fig. (31): Show Fe after corrosion by HCl (1M) without berry inhibitor.

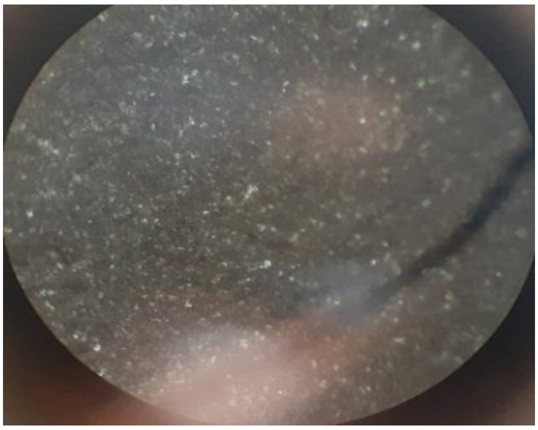

Fig. (32): Show Fe after corrosion by 1M HCl with berry inhibitor.

3.2. Effect of temperature

Weight loss-time curves of Cu in HNO_3 (1M) acid solution were studied in the temperature range (25- 45ºC). in the absence and presence of different concentrations of the extracts at different temperatures.

3.3. Effect of temperature on inhibition efficiency (%IE)

The inhibition efficiency (%IE) for Cu corrosion in the presence of various concentrations of the extracts and at different temperatures was obtained from Eq. (3).
The obtained weight-loss time curves are represented in. **Tables (2, 3)** illustrates the variation of % IE with extracts concentration at different temperatures. The obtained data revealed that:
The inhibition efficiency increased with an increase extract concentration. This suggests that the extract species are adsorbed on the copper/solution interface where the adsorbed species mechanically form a protected film on the metal surface which inhibits the action of the corrosion.
A decrease in the extract efficiency with increasing temperature were observed in case of mango inhibitor extract indicating that adsorption of extract species on Cu surface at these conditions is physical adsorption. An increase in the extract efficiency with increasing temperature were observed in case of berry leaves indicating that adsorption of extract species on Cu surface at these conditions is chemical adsorption. The effect of temperature on the inhibited acid-metal reaction is highly complex, because many changes happened on the metal surface like rapid etching and desorption of inhibitor and the inhibitor itself may undergo decomposition or re-arrangement.

Table (2): Variation of inhibition efficiencies (%IE) and surface coverage (θ) for various concentrations of mango inhibitor extract at different temperatures at 90 min immersion.

θ	% IE	(CR) mg/cm^2.min	Temp., °C	Conc., ppm
0.285	28.5	1.32	25	
0.251	25.1	1.99	30	
0.191	19.1	3.68	35	50
0.158	15.8	5.24	40	
0.095	9.5	7.35	45	
0.493	49.3	0.933	25	
0.414	41.4	1.56	30	
0.363	36.3	2.89	35	100
0.265	26.5	4.58	40	
0.204	20.4	6.45	45	
0.656	65.6	0.633	25	
0.618	61.8	1.02	30	
0.521	52.1	2.18	35	150
0.469	46.9	3.3	40	
0.418	41.8	4.73	45	
0.719	71.9	0.517	25	
0.665	66.5	0.892	30	
0.583	58.3	1.89	35	200
0.539	53.9	2.87	40	
0.425	42.5	4.68	45	
0.765	76.5	0.433	25	
0.737	73.7	0.7	30	
0.683	68.3	1.44	35	250
0.664	66.4	2.09	40	
0.476	47.6	4.26	45	
0.828	82.8	0.317	25	
0.784	78.4	0.575	30	
0.758	75.8	1.1	35	300
0.685	68.5	1.97	40	
0.671	67.1	2.68	45	

Table (3): Variation of inhibition efficiencies (% IE) and surface coverage (θ) for various concentrations of berry leaves extract at different temperatures at 90 min immersion.

θ	%IE	(CR) $mg/cm^2.min$	Temp. ◦C	Conc., ppm
0.575	57.5	0.783	25	
0.627	62.7	0.992	30	
0.655	65.5	1.567	35	50
0.687	68.7	1.95	40	
0.748	74.8	2.05	45	
0.624	62.4	0.692	25	
0.655	65.5	0.912	30	
0.686	68.6	1.425	35	100
0.715	71.5	1.775	40	
0.778	77.8	1.808	45	
0.670	67.0	0.608	25	
0.687	68.7	0.833	30	
0.721	72.1	1.267	35	150
0.748	74.8	1.567	40	
0.800	80.0	1.625	45	
0.692	69.2	0.567	25	
0.715	71.5	0.758	30	
0.748	74.8	1.142	35	200
0.776	77.6	1.391	40	
0.823	82.3	1.442	45	
0.719	71.9	0.517	25	
0.749	74.9	0.667	30	
0.771	77.1	1.042	35	250
0.806	80.6	1.208	40	
0.847	84.7	1.242	45	
0.742	74.2	0.475	25	
0.774	77.4	0.60	30	
0.794	79.4	0.933	35	300
0.827	82.7	1.075	40	
0.865	86.5	1.11	45	

3.4. Effect of temperature on copper corrosion rates (CR)

Dissolution degree depends on the area of the metal surface exposed and the time of detection, the corrosion quantity is given as respect to area(cm^2) and time(s). The quantity of corrosion result, or corrosion rate, is thus a basic calculation in corrosion. Corrosion rates (CR) can be meanly measured by either the concentration of metals dissolved in solution by chemical analysis method by eq. (2).

In **Tables (4, 5)** represent the corrosion rates of copper in 1M HNO_3 without and with six different concentrations of extracts at five different temperatures (25-45). As observed from the tabulated data, a remarkable decrease in copper corrosion rates was observed with the addition of increasing amount of the investigated extracts at each studied temperature. It is also clear that corrosion rate of copper i without and with extracts obeys Arrhenius type equation as it increases with raising solution temperature. These tables also, explain the berry extraction inhibitor is better than the mango extraction inhibitor at all different concentration, and different temperature.

Table (4): copper corrosion rates after 90-minute immersion in 1M HNO_3 without and with different concentrations of Mango inhibitor extract at different temperatures.

Conc. ppm	$CR \times 10^2$ ($mg.cm^{-2}.min^{-1}$)				
	25Cº	30Cº	35Cº	40Cº	45C⁰
Blank	2.0	3.0	5.0	6.9	9.0
50	1.5	2.2	4.1	5.8	8.2
100	1.0	1.7	3.2	5.1	7.2
150	0.7	1.1	2.4	3.7	5.3
200	0.6	1.0	2.1	3.2	5.2
250	0.5	0.8	1.6	2.3	4.7
300	0.4	0. 6	1.2	2.2	3.0

Table (5): Cu corrosion rates after 90-minute immersion in HNO_3 (1M) without and with different concentrations of berry leaves extract at different temperatures.

Conc. ppm	$CR \times 10^2$ ($mg.cm^{-2}.min^{-1}$)				
	25Cº	30Cº	35Cº	40Cº	45C⁰
Blank	2.0	2.9	5.0	6.9	9.0
50	0.9	1.1	1.7	2.2	2.3
100	0. 8	1.0	1.6	2.0	2.1
150	0. 7	0. 9	1.4	1.7	1.8
200	0. 65	0. 8	1.3	1.5	1.6
250	0. 6	0. 7	1.2	1.3	1.4
300	0. 5	0. 68	1.0	1.2	1.3

Table 6 The performance and experimental conditions of some previously reported natural-based corrosion inhibitors and berry and mango inhibitors.

Inhibitor	Optimum conc./ Material/ Solution	Highest (%IE)	Ref.
Tunbergia fragrans	500 ppm/ Mild steel/ 1.0 M HCl	81.0	[31]
Magnolia grandiflora	500 ppm/ Q235 steel/1.0 M HCl	85.0	[32]
Pterocarpus santalinoides leaves extract	0.7 g/L/ Carbon steel/1.0 M HCl	85.2	[33]
Opuntia elatior fruit	500 mg/L/ Mild steel/1.0 M HCl	79.7	[34]
Rosa canina fruit extract	800 ppm/ Mild steel/1.0 M HC	86	[35]
Taxus baccata extract	600 ppm/ Mild steel/ 1.0 M HCl	83	[36]
Haematostaphis barteri Leaves Extract	40 g/L/ Mild steel/ 1.0 M HC	73	[37]
Elaeoselinum thapsioides	900 ppm/Carbon steel	82	[38]
butanolic extract AVU	1.0 M HCl 700 ppm / Mild steel/ 1.0 M HCl	84	[39]
Berry, and mango extract	1.0 M HCl & 1.0 M HNO_3 / 300ppm/ carbon steel/	86.5	This work

4.Conclusion:

Two natural products extracted from berry leaves and mango leaves, as it was proven through the study that they are able to resist the corrosion of copper and iron metallic, and oil tubes made of iron alloys. From the data and results explain the berry extraction is a good inhibitor for the metal studies than mango extraction inhibitor. Corrosion rate with inhibitors were compared to the corrosion rate without inhibitor, also, the effect of temperature on its adsorption and wear rate.

Acknowledgement

We thank of El-Khalij oil company in Elwahate Jalu, Libya for aid and cooperation to complete this paper. We also thank of an engineering and workers of El-Khalij oil company for the cooperation and aids.

5. References

[1]- Xu, Y.& Tan, M. Y. (2019), Probing the initiation and propagation processes of flow accelerated corrosion and erosion corrosion under simulated turbulent flow conditions, *Corrosion Science*, 151: 163-174.

[2]- Alrashed, M.M. Jana, S. and Soucek, M.D. (2019), Corrosion performance of polyurethane hybrid coatings with encapsulated inhibitor, *Progress in Organic Coatings*, 130: 235-243.

[3]- Man, C. Dong, C. Kong, D. Wang, L. and Li, X. (2019), Beneficial effect of reversed austenite on the intergranular corrosion resistance of martensitic stainless steel, *Corrosion Science*, 151: 108-121.

[4]- Fang, Y. Suganthan, B. Ramasamy, R. P. (2019), Electrochemical characterization of aromatic corrosion inhibitors from plant extracts, *Journal of Electroanalytical Chemistry*, 840: 74-83.

[5]- Guo, X. Fan, Y. Gao, W. Tang, R. and Zhang, L. (2019), Corrosion resistance of candidate cladding materials for supercritical water reactor, *Annals of Nuclear Energy*, 127: 351-363.

[6]- Wu, Y. Zhu, X. Zhao, W. Wang, Y. Xue, Q. (2019), Corrosion mechanism of graphene coating with different defect levels, *Journal of Alloys and Compounds*, 777: 135-144.

[7]- Chen, H. Hou, X. He,J. Guo, H. (2019), Bioxidant corrosion behaviour of CoNiCrAlY coated IN738 at 1100 °C, *Corrosion Science*, 151: 154-162.

[8]- Mędrala, A. M. Magdziarz, A. Kalemba-Rec, I. and Nowak, W. (2019), "The influence of potassium-rich biomass ashes on steel corrosion above 550 °C, *Energy Conversion and Management*, 187, 15-28.

[9]- Morończyk, B. Ura-Bińczyk, E. Kuroda, S. Jaroszewicz, J. and Molak, R. M. (2019), Microstructure and corrosion resistance of warm sprayed titanium coatings with polymer sealing for corrosion protection of AZ91E magnesium alloy, *Surface and Coatings Technology*, 363: 142-151.

[10]- Arora, S. and Srivastava, C. (2019), Microstructure and corrosion properties of Ni- Co-graphene oxide composite coatings, *Thin Solid Films*, 677: 45-54.

[11]- Liu, C. T. Fischer, K. B. and Rochelle, G. T. (2019), Corrosion of carbon steel by aqueous piperazine protected by $FeCO_3$, *International Journal of Greenhouse Gas Control*, 85: 23-29.

[12]- Trolic, I.M. Serdarevic, N.L. Todoric, Z. Budimir, A. and Curkovic, H.O. (2019), Corrosion of orthodontic arch wires in artificial saliva in the presence of Lactobacillus reutter, *Surface and Coatings Technology, in press, accepted manuscript,*

[13]- Kumar Das, J. Pradhan, B. (2019), Effect of cation type of chloride salts on corrosion behaviour of steel in concrete powder electrolyte solution in the presence of corrosion inhibitors, *Construction and Building Materials*, 208: 175-191.

[14]- Duffó, G.S. Farina, S.B. and Schulz F.M. (2019), Corrosion behaviour of non-ferrous metals embedded in mortar, *Construction and Building Materials*, 210: 548-554.

[15]- Golchinvafa, A., Anijdan, S. M., Sabzi, M., & Sadeghi, M. (2020). The effect of natural inhibitor concentration of Fumaria officinalis and temperature on corrosion protection mechanism in API X80 pipeline steel in 1 M H_2SO_4 solution. *International Journal of Pressure Vessels and Piping*, 188, 104241.

[16]- Abdallah, M., Altass, H. M., Al-Gorair, A. S., Al-Fahemi, J. H., Jahdaly, B. A. A. L., & Soliman, K. A. (2021). Natural nutmeg oil as a green corrosion inhibitor for carbon steel in 1.0 M HCl solution: Chemical, electrochemical, and computational methods. *Journal of Molecular Liquids*, *323*, 115036.

[17]- Nardeli, J. V., Fugivara, C. S., Taryba, M., Pinto, E. R., Montemor, M. F., & Benedetti, A. V. (2019). Tannin: A natural corrosion inhibitor for aluminum alloys. *Progress in Organic Coatings*, *135*, 368-381.

[18]- Pradipta, I., Kong, D., & Tan, J. B. L. (2019). Natural organic antioxidants from green tea form a protective layer to inhibit corrosion of steel reinforcing bars embedded in mortar. *Construction and Building Materials*, *221*, 351-362.

[19]- Halambek, J., Cindrić, I., & Grassino, A. N. (2020). Evaluation of pectin isolated from tomato peel waste as natural tin corrosion inhibitor in sodium chloride/acetic acid solution. *Carbohydrate polymers*, *234*, 115940.

[20]- Wang, H., Gao, M., Guo, Y., Yang, Y., & Hu, R. (2016). A natural extract of tobacco rob as scale and corrosion inhibitor in artificial seawater. *Desalination*, *398*, 198-207.

[21]- Abdel-Gaber, A. M., Abd-El-Nabey, B. A., Khamis, E., & Abd-El-Khalek, D. E. (2011). A natural extract as scale and corrosion inhibitor for steel surface in brine solution. *Desalination*, *278*(1-3), 337-342.

[22]- Soltani, N., Tavakkoli, N., Kashani, M. K., Mosavizadeh, A. E. E. O., Oguzie, E. E., & Jalali, M. R. (2014). Silybum marianum extract as a natural source inhibitor for 304 stainless steel corrosion in 1.0 M HCl. *Journal of Industrial and Engineering Chemistry*, *20*(5), 3217-3227.

[23]- Pal, A., & Das, C. (2021). New eco-friendly anti-corrosion inhibitor of purple rice bran extract for boiler quality steel: Experimental and theoretical investigations. *Journal of Molecular Structure*, 131988.

[24]- Radojčić, I., Berković, K., Kovač, S., & Vorkapić-Furač, J. J. C. S. (2008). Natural honey and black radish juice as tin corrosion inhibitors. *Corrosion Science*, *50*(5), 1498-1504.

[25]- Abdel-Gaber, A. M., Abd-El Nabey, B. A., Khamis, E., Abdelattef, O. A., Aglan, H., & Ludwick, A. (2010). Influence of natural inhibitor, pigment and extender on corrosion of polymer coated steel. *Progress in Organic Coatings*, *69*(4), 402-409.

[26]- Suliman, M., Alkilani, M., Abdullah, T., & Ali, M. (2019). The Effect of Methyle Carbazodithoate" Corrosion inhibitor on Corrosion Behaviour of Low Carbon Steels in Acid Solution at Different Temperatures. *Journal of Pure & Applied Sciences*, *18*(4).

[27]- Suliman, M. S., Almadani, M. A., & Ahmied, E. K. (2019). The Inhibition of Mild Steel Corrosion by Sulphur Containing Organic Compound. *Journal of Pure & Applied Sciences*, *18*(2).

[28]- Khalifa, S., AL-abbassi, A., & Suliman, M. (2018). Adsorption and Corrosion Inhibition of Mild Steel in Acidic Media by Expired Pharmaceutical Drug. *Journal of Pure & Applied Sciences*, *17*(4).

[29]- Al-abbasi, A., & Shana, I. E. (2021). Corrosion Inhibition of Mild Steel in Acidic Media by Expired Carbimazole Drug. *Journal of Pure & Applied Sciences*, *20*(2), 176-180.

[30]- Almahdi, O., & Almassri, O. (2021). Corrosion Inhibition characteristics of Reinforced Steel in H_2SO_4 by benzoyl Thiourea. *Journal of Pure & Applied Sciences*, *20*(2), 137-141.

[31]- Muthukumarasamy, K., Pitchai, S., Devarayan, K., & Nallathambi, L. (2020). Adsorption and corrosion inhibition performance of Tunbergia fragrans extract on mild steel in acid medium. *Materials Today: Proceedings*, *33*, 4054-4058.

[32]- Chen, S., Chen, S., Zhu, B., Huang, C., & Li, W. (2020). Magnolia grandiflora leaves extract as a novel environmentally friendly inhibitor for Q235 steel corrosion in 1 M HCl: Combining experimental and theoretical researches. *Journal of Molecular Liquids*, *311*, 113312.

[33]- Ahanotu, C. C., Onyeachu, I. B., Solomon, M. M., Chikwe, I. S., Chikwe, O. B., & Eziukwu, C. A. (2020). Pterocarpus santalinoides leaves extract as a sustainable and potent inhibitor for low carbon steel in a simulated pickling medium. *Sustainable Chemistry and Pharmacy*, *15*, 100196.

[34]- Loganayagi, C., Kamal, C., & Sethuraman, M. G. (2014). Opuntiol: An active principle of Opuntia elatior as an eco-friendly inhibitor of corrosion of mild steel in acid medium. *ACS Sustainable Chemistry & Engineering*, *2*(4), 606-613.

[35]- Sanaei, Z., Ramezanzadeh, M., Bahlakeh, G., & Ramezanzadeh, B. (2019). Use of Rosa canina fruit extract as a green corrosion inhibitor for mild steel in 1 M HCl solution: A complementary experimental, molecular dynamics and quantum mechanics investigation. *Journal of industrial and engineering chemistry*, *69*, 18-31.

[36]- Hanini, K., Merzoug, B., Boudiba, S., Selatnia, I., Laouer, H., & Akkal, S. (2019). Influence of different polyphenol extracts of Taxus baccata on the corrosion process and their effect as

additives in electrodeposition. *Sustainable Chemistry and Pharmacy*, *14*, 100189.

[37]- Ishak, A., Adams, F. V., Madu, J. O., Joseph, I. V., & Olubambi, P. A. (2019). Corrosion inhibition of mild steel in 1M hydrochloric acid using Haematostaphis barteri leaves extract. *Procedia Manufacturing*, *35*, 1279-1285.

[38]- Benahmed, M., Selatnia, I., Djeddi, N., Akkal, S., & Laouer, H. J. C. A. (2020). Adsorption and corrosion inhibition properties of butanolic extract of Elaeoselinum thapsioides and its synergistic effect with Reutera lutea (Desf.) Maires (Apiaceae) on A283 carbon steel in hydrochloric acid solution. *Chemistry Africa*, *3*(1), 251-261.

[39]- Zaher, A., Aslam, R., Lee, H. S., Khafouri, A., Boufellous, M., Alrashdi, A. A., ... & Ouhssine, M. (2022). A combined computational & electrochemical exploration of the Ammi visnaga L. extract as a green corrosion inhibitor for carbon steel in HCl solution. *Arabian Journal of Chemistry*, *15*(2), 103573.